Journal of Materials Chemistry A

Carbonaceous materials as a situated for conventional Dye-sensitized Solar Cells counter electrode

Journal:	*Journal of Materials Chemistry A*
Manuscript ID:	TA-REV-04-2015-002840.R1
Article Type:	Review Article
Date Submitted by the Author:	02-Aug-2015
Complete List of Authors:	Ghorbani Shiraz, Hamid; University of Tehran, Razi Astaraie, Fatemeh; University of Tehran,

Journal Name

ARTICLE

Carbonaceous materials as a situated for conventional Dye-sensitized Solar Cells counter electrode

Received 00th January 20xx,
Accepted 00th January 20xx

DOI: 10.1039/x0xx00000x

www.rsc.org/

H. Ghorbani Shiraz [a], F. Razi Astaraie[b]

According to precipitation growth in energy demand, renewable energy plays a great role in both economic and energy supply. Recently, Solar cells which convert solar energy to electricity have been proposed as typical devices in this regard. Dye-sensitize solar cells as a third generation of solar cells have attracted more attentions. Counter Electrodes as one of the key components in electron cycling and redox reaction (to regenerate oxidized electrolyte), have faced several challenges such as high price, and complicate deposition process of conventional Platinum electrode. As cost effective devices, scientists have proposed carbonaceous materials as Pt alternatives that satisfy catalytic role. In this paper, carbonaceous materials as counter electrode are reviewed. Carbon structures present high surface area as well as low impedance which lead to efficient solar cells. The improvements occur through porosity or nanostructure which is proposed by the material morphologies; in this regard, some disadvantages which respect to the fabrication procedure, also are included.

Keyword: Counter electrode; Carbon nanostructures; Platinum

I. Introduction

Energy as the most challengeable problem demonstrates effective role in countries guideline. Fossil fuels as the primary source of energy encounter several problems such as environmental damages, as well as non-renewability. On the other hand, renewable sources have been emerged as remedy to both energy and environmental concerns [1-10]. Amongst, the most effort has focused on solar as an interminable resource. According to high price of fabrication and upkeep facilities of conventional solar cells, cost-effective approaches have defined new configurations of solar cell. Gratzel et al. combined nanostructure electrodes and charge injection dye as first Dye-sensitized Solar Cell (DSSC) by conversion efficiency more than 7% [11]. DSSC consist of working electrode (photoanode) like TiO_2 nanostructure, sensitizer dye, redox electrolyte like iodide/tri-iodide (I^-/I_3^-), and photocathode, so-called counter electrode. Facility in fabrication procedure, low cost materials, and relative flexibility has provided a considerable potential with these devices. Dye as sensitizer usually is prepared based on Ruthenium Polypyridine complex, due to wide recognition on optical attitude and photo-redox reactions [12].

DSSCs insert by two film layers which usually are made of transparent conductive oxide (TCO) such as fluorine-doped tin oxide (FTO). Both transparency and conductivity are necessary for these films [13]. One of the key components of working electrode is semiconductor. TiO_2 is more common semiconductor due to favourable optical feature [14]. Using porous structures like nanoporous films significantly increase available surface area for dye molecules bonding, but limit the electron transfer rate, simultaneously.

The Counter Electrode (CE) is a decisive factor in power conversion efficiency (PCE); due to cathode role which implies the reduction of oxidized species of electrolyte. Electrolyte consists of a couple of ions that transform to each other through electron exchanging (redox reactions). Iodide/tri-iodide (I^-/I_3^-) is one of the best-known electrolytes for researchers; however, there is some shortcomings with this: toxicity and volatility. Liquid electrolyte is not stable in wide range operation temperatures of solar cell typically deal with. As a remedy, high-mobile solid electrolytes are being investigated (solid-state dye sensitized solar cell).

Generally, CEs should possess some special characteristics. Amongst, it can be referred to high conductivity and catalytic activity, due to regeneration the oxidized species of electrolyte [15]. Conventionally, Platinum (Pt) as catalysis is deposited over TCO. It is clear that Pt morphology, which directly introduces available surface area, will impress the number of catalytic sites; however, from viewpoint of economy Pt is unfavourable choice. Researches intensively have been investigated to find promise alternative which possess Pt characteristics also cost effective.

In this paper, firstly the performance of a DSSC and applied different structures of Pt have been reviewed. Then we have focused on carbonaceous materials as remedy to conventional Pt electrodes.

[a] School of Chemical Engineering, University of Tehran, Tehran, Iran
[b] Faculty of New Sciences and Technologies, University of Tehran, Tehran, Iran

Corresponding Author:
Dr. Fatemeh Razi Astaraie
Email: razias_m@ut.ac.ir
Tel: +98-216 111 85 75

II. Brief in electron transfer in DSSCs

When DSSC exposes to the sun light, dye molecules absorb photon's energy. The photons which possess energy content equal to the gap of HOMO-LUMO are absorbed. It excites electron to the HOMO band in dye molecules, then the electrons are injected to conduction band (CB) of semiconductor. The charge transfer is done in timescale of tens femtosecond- to hundreds picoseconds. Dye is stabilized to the ground state through the help of electrolyte; i.e. in the case of iodide/tri-iodide (I^-/I_3^-), iodide (I^-) will be oxidized to tri-iodide (I_3^-) according to $3I^- \leftrightarrow 2e^- + I_3^-$; which the reduction of (I_3^-) is accomplished by CE. So the resulted electrons are consumed in dye ground state process. The electrons which have been injected in the semiconductor CB are cumulative in micro- to millisecond range. Consequently, electrons can leave the photoanode and follow to the CE through external circuit [16, 17]. Thus, CE must be prepared to provide low electron transfer resistance also contribute rapid reduction of oxidized electrolyte. With this in mind, CE has great role to continue the electron cycle.

As a considerable issue, recombination of electrons imposes detrimental effect on PCE. Mainly, electrons back transfers lead to recombination. Unfortunately electron collecting in working electrode occurs slower than exciting in dye molecule; therefore there always is partial electron cumulatives especially at the interface of semiconductor/dye/electrolyte and most of the time result in recombination. Chiefly, electron recombinations happens by electrolyte and oxidized dye in mili- to a second and micro- to millisecond, respectively. Also, recombination comes from shuffle electrons could be considerable; thereby geometry of semiconductor plays an important role to charge transfer.

More recently, researchers have proposed given structures for the semiconductor included nanowires and quantum dots (QDs) which are introduced significant enhancement on the conversion efficiency [18].

III. Platinum

Pt has been defined as one of the best CE and this is due to possess of given properties that are requisite for each CE such as stability in air or water even at high temperatures (does not oxide), good electrical and thermal conductivity [19, 20 and 21], etc. On the other hand, it also possesses some disadvantages like high cost, low abundance of material, diminishing catalytic property in the exposure of dye molecule, and hardness (vacuum conditions) of conventional method of sputtering. These undesirable features simulate the efforts to find an alternative CE in DSSCs [22, 23].

The conventional CEs which are prepared based on deposition of Pt on the substrate (TCO) possess significant electrocatalytic activity [24]; electro- refers to electrical conductivity and catalytic refers to application as catalyst in reduction of oxidized electrolyte. The activity varies on the different morphology; e.g., compared to Pt film, nanostructure can promote activity by a range of ways such as (a) higher surface area, thus higher catalytic sites, (b) decrease charge transfer resistance (CTR), (c) higher transparency, due to size reduction [25]. However, the employed method**,** such as doctor-blade technique, screen-printing, spray-coating, etc. can result in different morphology and different activity.

Some configurations result in unfavourable mechanical cohesion and/or high series resistance. Also, CTR occurs due to contact quality between catalytic particles boundary and conductive substrate, which varies in each morphology and structure**.**

It was mentioned that regard to CE structure, high surface area plays a great role on the cell performance. It is clear that broad surface area supplies the large number of catalytic active sites. Kim et al. [26] proposed high surface area in the structure of Pt CE through Pt hollow sphere over both bare and Pt sputter FTO (II). Electrochemical Impedance Spectroscopy (EIS) and I-V measurement revealed that compared to conventional sputtering electrode, the performances were improved. The results have been compared in Table 1. The characterizations demonstrated that the approaches cause by facility in electron transfers through broad surface area; especially for the sample of II. Thereby, increase in fill factor (FF) and short circuit current (I_{SC}) resulted in higher efficiencies.

Choi et al. [27] prepared Pt nanoparticles by thermal degradation method and investigated the effect of transparent Pt CE on the cell performance. They concluded that the PCE influences by heating rate. It is attributed to electrocatalytic activity of the sample. It corresponds to morphology of Pt nanoparticle that was provided via given degradation rate. Fig. 1 shows the effect of thermal degradation in different morphologies. It was resulted that the rate of 1.2 ◦C min^{-1} offers the highest surface area. Indeed, this heating rate enhanced PCE through introduction of numerous catalytic sites.

Table 1 Comparison of Pt decorated counter electrode

Item	CTR (Ωcm^2)	PCE (%)
I	0.91	8.2
II	0.48	8.53
Conventional	1.28	7.89

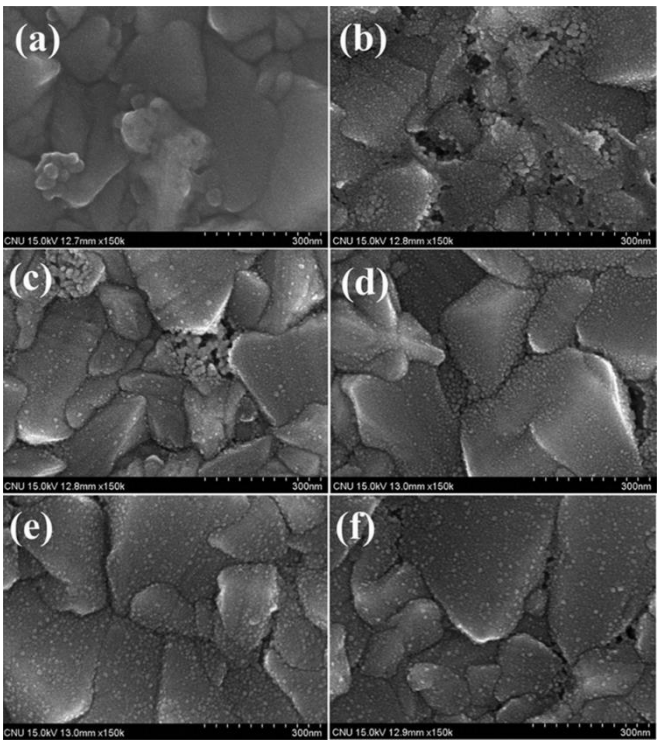

Fig. 1 HRSEM images of Pt-NPs CEs prepared by thermal degradation method with different heating rate during sintering process: (a) 3 ◦C min^{-1}, (b) 2 ◦C min^{-1}, (c) 1.5 ◦C min^{-1}, (d) 1.2 ◦C min^{-1}, (e) 1 ◦C min^{-1} and (f) 0.85 ◦C min^{-1}; the sample (d) shows broad and distinctive surface area [27].

Yang et al. [28] prepared CE by pulse electrode deposition method. The characterization of fabricated sample demonstrated significant surface roughness, compare to the reference sputtered samples. The cyclic voltammetry (CV) revealed higher catalytic activity rather sputtered Pt electrode. Also, it was proved that pulse-plated electrode revealed the PCE of 6.0% much more than that of sputter, as they expected. Also, lin et al. [29] examined the effect of morphology by Platinum nanotubes (PNTs) grown on FTO substrate using facile polycarbonate template. EIS measurements indicated that the PNTs as highway for electron transfer possess higher electrocatalytic activity for electrolyte redox reduction, compared to conventional Pt CE (Fig. 2). These morphology resulted in PCE of 9.05% under 100 $mWcm^{-2}$ simulated solar light; while the reference sample (spin-coat) revealed the efficiency of 7.24.

Zhao et al. [30] incorporated the low cost surfactant in order to prepare better adhesion of Pt materials to substrate and introduction screen-printing Pt CEs. In this regard, they proposed DSSCs based on screen-printed, spin-coating and dip-coating. The PCE of 7.30%, 7.03% and 6.96% obtained for screen printed, spin-, and dip coating, respectively. The characterizations explained the improvement of screen-printed CE on both morphology and CTR. In the case of competitive sample, uniformity in distribution of Pt particles has introduced numerous local catalyses. On the other hand, CV and EIS measurements showed that the CTR for the screen-printed CE assessed as the lowest. So, the reduction reaction could be defined in fast rate.

Recently, Pt composites have been defined as novel CEs. Tau et al. [31] made a composition of Pt and silicon nanowires (SiNWs) by electroplating method. The fabricated one exhibited higher electrochemical activity, compared to sputtered Pt CE. The higher performance was emerged on PCE of 8.30%, in front of 7.67% for sputter one. It is ascribed to the promotion in CTR which improved notably, 0.5%. In fact, nanowire defined as an oriented electron exchange system and the Pt as redox reaction center.

Also, fabrication conditions have been emerged impressive. Yu et al. [32] synthesized novel DSSCs using FTO nanocrystals as a substrate to deposit Pt. It resulted in PCE of 6.09%. Obviously, uneven substrate present higher surface to allow the Pt species, rather smooth level. On the other study, Meng et al. used the press-transfer method to prepare Pt CE. The DSSC using the Pt CE under different applied pressures, achieved to the PCE of 7.21 (100 MPa) and 5.51% (50 MPa) [33]. It shows that higher pressures can result in higher efficiency. It may refer to charge transformation; i.e. compact media introduces facile charge transformation through reduction in contact resistance; thereby the catalytic activity can be defined in higher quality.

As assigned before, Pt may be replaced by some other alternative due to a number of limitations like price. As stated the morphology can take into account as a decisive factor. Indeed, it can affect the performance through reduction in CTR and introduction of more catalytic sites.

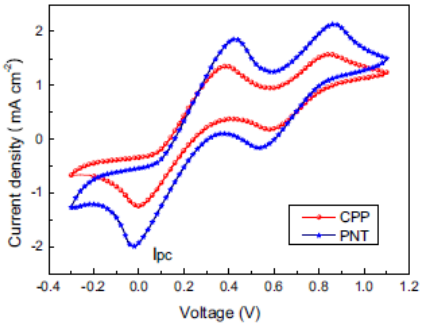

Fig. 2 CV for PNT and CPP electrodes [29].

Recently, carbonaceous materials such as carbon black, mesoporous carbon, and a numbers of well-known carbon nanostructures like carbon nanotubes (CNTs) and graphene which have demonstrated great catalytic activity have been proposed as promise candidate for CE. Following, the recent progresses and their advantages has been reviewed. First, theory analysis of the materials, with the focusing on CTR, is brought and then they will be discussed one by one.

IV. Carbon materials

Carbon nanomaterials are promising candidates to replace conventional Pt electrodes because of the advantages such as low cost, high catalytic activity, high electrical conductivity, high thermal stability, and good corrosion resistance; e.g., Individual carbon nanotubes can be electrically high conductive, mechanically strong and also offer flexibility toward bending.

1. Charge-transfer resistance and Catalytic activities

a) Carbon nanomaterial as counter electrode [34]

The key characteristic of the DSSC CE is the CTR. CTR can be measured by EIS, and it should be as low as possible. In the case of porous carbon nanomaterials CE, CTR (notified by R_{CE} ($\Omega.m^2$) in the equations) decreases as film thickness d increases;

$$R_{CE} = r_{CE}.d^{-1} \qquad (1)$$

Where r_{CE} ($\Omega.m^3$) demonstrates charge transfer resistance per unit volume of the film. This has been supposed that the whole film contribute in the charge transfer process; however, it is an ideal electrode. Since, the ideal performance may not be satisfied; the modification will be considered, following.

r_{CE} can be described on the function of electrode microstructure characterizes, such as specific surface area per unit volume A_V ($m^2.m^{-3}$) and the charge transfer resistance per surface unit area, $r_{CE,A}$ ($\Omega.m^2$);

$$r_{CE} = r_{CE,A}.A_V^{-1} \qquad (2)$$

It was notified that a fraction of (specific) surface area would be contributed in charge transfer process. One criterion of catalytic activity is electrode capacitance C_{CE} ($F.m^{-2}$), which has defined by following equation;

$$C_{CE} = c_{CE}.d = c_{CE,A}.A_V.d \qquad (3)$$

Where c_{CE} and $c_{CE,A}$ are the capacitances per unit volume ($F.m^{-3}$) and per surface area ($F.m^{-2}$) of the electrode microstructure, respectively. Taking product of the charge transfer resistance and the capacitance leads to a proper measurement of area, regardless of BET technique and other complex methods;

$$R_{CE}.C_{CE} = r_{CE,A}.c_{CE,A} \qquad (4)$$

The latter equation satisfies the lack of thickness (d) and specific surface area per unit volume (A_V (m^2/m^3)); which is arduous to find for micro- and nanostructures. It is a suite comparison criterion for catalytic activities. The relation suggests that ideal electrode is defined as high capable in transferring and accepting the electrons. Carbonaceous as high useable materials in industrial batteries satisfy both attitudes. Also, escalation applications in the photocatalytic processes confirm this claim.

For different carbon nanomaterials, authors have assumed that their area-specific capacitances $c_{CE,A}$ value are equal. $c_{CE,A}$ is defined as the value which depends only on the capacitance of boundary double layer per microscopic surface area. The boundary double layer is included in the interface of electrolyte and CE, where charge transfer occurs. With this in mind, it is clear that catalytic activity of the materials can be optimized by introducing electrodes defined nanostructure material to enhance available surface sites; i.e., extend boundary double layer, due to enhance electrically active surface and preparing continuum media to charge transfer. The preferable value for CTR is in order of 1 $\Omega.cm^2$ that has obtained with optimized planar Pt CE; similar to those of some CNT electrodes or carbon nanoparticle electrodes with several micrometers in thickness. It demonstrates the potential of the carbon nanomaterial CEs, properly.

In addition, durability to bending has supplied by employing carbonaceous materials and this signalizes the application of carbonaceous toward flexible DSSCs.

2. Carbon black

Carbon black is produced as by-product of incomplete combustion and has variety properties such as high area to volume ratio and electrocatalytic activity; which has been known as a good candidate for CEs. In carbon black and other carbonaceous materials, the active sites for catalysis have located at the edge crystals [35, 36 and 37].

When carbon materials are used as the CEs, surface morphology can play as a great role. In this regard, Takahashi et al. [38] have demonstrated that roughness possesses important effect on the efficiency. They showed that as roughness factor increases, the CTR decreases and thereby the performance improves. Also, it was demonstrated that, there must be a control on the layer thickness because it effects on the catalysis and resistance parameters, strongly; however, the dominant nature of carbon materials, amorphous, could be helpful to this challenge.

In general, the CEs thickness should be kept below few tens of microns, which is typical optimum thickness of the free electrolyte layers, regard to the planar Pt CE [34]. Gratzel et al. [39] employed carbon black as the CE on FTO substrates. They studied the thickness of carbon black as the CE. According to the research, 14.47 µm thickness of carbon black as CE, exhibited an efficiency of 9.1% and significant current density and open circuit voltage. From the EIS measurements, it was demonstrated that the broad surface area in carbon black structure revealed a low CTR around 2.96 Ωcm^2. They proved that thickness of 10 µm carbon black offers optimum point to take the maximum fill factor and PCE. They observed as the thickness increases, CTR decreases; and above few tens of microns, PCE became one-third of conventional Pt.

Also amorphous carbon as flexible CE has been used, recently. Bojan et al. [40] dispersed carbon powder with average particle size less than 50 nm in ethanol, ultrasonically; and solution was spray coated over FTO substrate. Carbon thickness were controlled by means of variety in deposition time from 10 s to 420 s. SEM images showed pores size around of few angstroms, which is accessible to diffusion and the reduction reaction of oxidized species. Characterizes were done by EIS and CV (Fig. 3). CTR of carbon CE, which had been sprayed for 420 s, defined at the same order of platinized. Peak tails on the left relate to the reduction of tri-iodide. CV indicates that the catalytic behaviour of the carbon electrode has been emerged comparable to that of Pt ones. It was determined that definition of spray coating layer introduces porous structure and each particle develops catalytic activity by itself. Due to the lower surface area and low number of catalytic sites in carbon thin films, tri-iodide reduction rate was slowed. As result, thinner films (short deposition time) can result in low current density which comes from high level of CTR; however, it is confirmed by the EIS measurements.

Addition to crystallography and thickness, purity takes to account as a decisive factor in the performance. Pure carbon materials which have been employed as CEs, exhibited very low series resistance and CTR; consequently high conductivity and high catalytic properties could be expected [41].

Other factors contribute on cell performance through different effects such as morphology and particle size, deposition method. However, the result of morphology and particle size is offered by deposition method, strongly.

Joshi et al. [42, 43] used carbon nanoparticles (< 50 nm) with TiO_2, as binder, to form a catalytic CE for DSSC. Carbon nanoparticles were treated in the mixture of TiO_2 and water. The obtained mixture was treated in form of paste. It was spin-coated over FTO as CE. Surface characterization demonstrated that the particles size in carbon/TiO_2 composite film were larger than those for pure TiO_2. Compared to 6.4% of PCE with platinized device, the fabricated DSSC exhibited PCE of 5.5%. Lower efficiency of the DSSC is ascribed to higher series resistance rather conventional Pt electrodes. It evaluated due to large thickness and resistivity of carbon structure. Also large grain size through surface area influences on the efficiency.

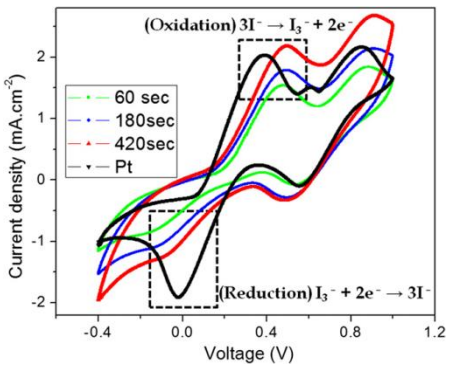

Fig. 3 CV obtained at a scan rate of 50 mV s-1 for the reduction of tri-iodide with the carbon (spray coated for 60, 180, 420 s) and Pt electrode [40].

As resulted before, porosity which extends available surface area, leads to increase in electrocatalytic sites; thereby better redox reduction will be obtained. On the other hand, large size particles which result in low surface to volume ratio have detrimental effects on the electrochemical property. So, surface catalytic activity drops and redox reduction rate substantially decreases. According to significant series resistance of typically two times higher than that of platinum electrode, it seems that former effect (large particle size) is important (rather porosity) for photovoltaic parameters.

Another study refers to Chen et al. research [44]. They dispersed carbon black in aqueous solution and it was added to ethyl alcohol to form a paste. They defined 10 µm paste thickness on FTO substrate using Squeegee method. The characteristics revealed that PCE was round 4.0%; while the achieved value for sputtered Pt-based DSSC revealed the PCE of 6.13%. The lower efficiency may attribute to lower conductivity and relative large thickness. The structure avoids lower catalytic sites; also regard to thickness, it defines long electron pathway; which in turn, it has been introduced higher CTR.

Further step has been progressed by Elbohy et al. [8]. They investigated effect of carbon nanoparticles (CNPs) composite on DSSC performance by employing as support of Pt in CE. CNPs were soaked in platinum precursor solution. Next, it underwent post-treatment and finally resulted in the form of paste which was doctored blade over FTO substrate (10 µm thick). The fabricated electrode was dried at 60 °C for 12 h. As reference, Pt CE was prepared through spin coating on FTO. SEM images of Pt and CNPs/Pt were compared and proved that later one results in porous structure; while Pt sample offers smooth surface. CV characterizations (Fig. 4 top) were studied for both reference Pt and CNPs/Pt electrodes. Compared to the reference electrode, on the left tails, higher peak current density for the CNPs/Pt electrode indicates faster reduction of tri-iodide species. This states higher electrocatalytic activity of the CNPs/Pt electrode. The high reduction rate is attributed to larger surface area of the porous CNPs/Pt electrode which provides larger number of reduction sites and thus enhances the activity. On the other hand, the other peak tail shows the oxidation of iodide which has no significant effect on PCE. Also, they were examined the effect of CNPs/Pt thickness on solar cell parameters (Fig. 4 bottom). They employed 4 µm, 9 µm, 13 µm, and 22 µm as CE thickness. Proposed DSSCs underwent the characterizations under A.M 1.5 illumination of light intensity of 100 mW/cm^2. Although Short circuit current density (J_{sc}) and open circuit voltage (V_{oc}) did not show any clear correlation with thickness of CE, measurements revealed that the thicker samples demonstrate better performance in a number of parameters (FF, R_{se}, PCE and sometimes J_{sc} and V_{oc}). It explains no contradiction to the aforementioned arguments; i.e. high thickness of porous media could be translated as high surface area and conclusively high reaction centers.

Table 2 covers all found results; it obviously defines CNPs/Pt as proper alternative to conventional Pt.

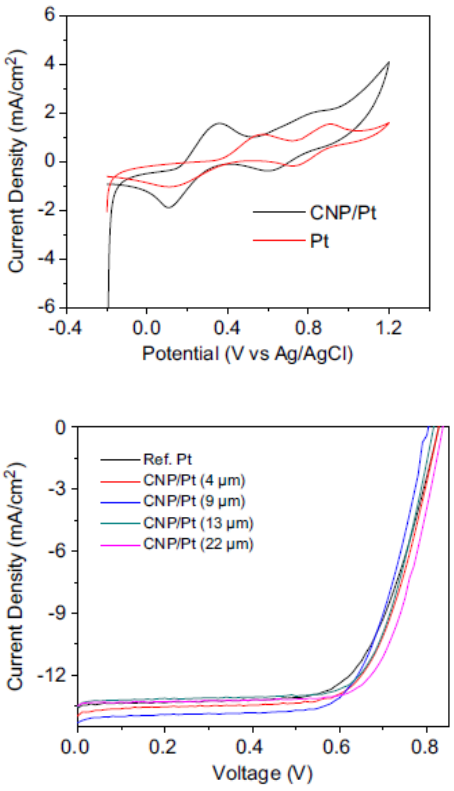

Fig. 4 CV of reference platinum, and carbon nanoparticle supported platinum (top); Photocurrent–voltage curves of DSSC with different counter electrodes (bottom) [8].

As a result, thickness, particle size, environment, and the composition can affect on the performance through various mechanism; however, the electrocatalytic activity and charge transfer rate are strongly purposed.

Table 2 Thickness and photovoltaic parameters for various CE thickness and reference ones

Thickness (µm)	J_{SC} (mA/cm^2)	V_{OC} (V)	FF (%)	PCE (%)	CTR (Ω cm^2)
4	13.98	0.83	0.68	7.87	10.12
9	14.23	0.80	0.69	7.86	9.53
13	13.53	0.82	0.70	7.67	9.38
22	13.49	0.84	0.72	8.12	8.99
Ref.	13.60	0.83	0.66	7.49	11.25

3. Carbon Nano Fiber

Along carbon nanostructure, carbon nanofibers (CNFs) have been employed in DSSCs. Limiting in surface area could be compensated by introducing high thickness which will lead to higher resistance and impedance, unfortunately. This is the shortcoming to these cost-effective matters. It may be synthesized in various diameters and length by chemical vapor deposition (CVD) or pyrolysis of electro-spun fibers; using organic matter as precursor.

Joshi et al. [45] prepared electro-spun carbon nanofibers (ECNs) and employed as CE. After the post-treatment they achieved to the paste which was doctored blade over FTO substrate. Top view SEM image (Fig. 5 left) of the ECNs demonstrates countless interconnection in

the mixed matrix. The rupture structure introduces numerous micropore which can be defined as a proper catalytic sites to redox reactions. The ECNs are defined relatively uniform with an average diameter of ~ 250 nm and tens of microns length. Reversely, top view SEM image of a ECNs CE (Fig. 5 right) shows that nanofibers length vary from submicron to micron; it translates that some of nanofibers has broken and made short length fibers during process. Apart from initial structural defects (in Fig. 5 left), the broken tips with the high charge density in the, lead to high rate recombination and low conductivity; yet higher surface area are provided.

Hierarchical types of carbon fiber (CF) were proposed to fabricate the CE by Yoo et al. [46]; carbon fiber (CF), NaOH etched carbon fiber (ECF), carbon fiber with thermally deposit platinum (CFPt), and carbon fiber etched with NaOH followed by thermal deposition of platinum (ECFPt); also a thermal Pt deposition was fabricated as reference electrode. It was demonstrated that etching and platinum deposition processes introduced roughness over the structures; available surface area got raised through efficient catalytic inequalities. EIS measurements were revealed that surface treatment, has improved catalytic performance of the carbon fiber CE. Fig. 6 shows the photovoltaic performance of the samples. In comparison to the reference, increase in V_{OC} comes at the expense of reduction in J_{SC}; this is expandable to all carbonaceous electrodes and reflected in bottom left. However, the Pt incorporation results in higher PCE by reduction in series resistance. Thus, the fabricated electrode did not meet comparable performance compared to FTO/Pt; (Fig. 6 bottom). Detrimental effect can be ascribed to the CFs dimention. Nanoscale component can define more efficient through high surface to volume ratio; as Joshi study [45].

Recently, highly graphitic carbon nanofibers (CNFs) were defined as suitable alternative to DSSCs CE [47]. The CNFs were grown by introducing pure methane to the Ni-based catalyst at four temperatures from 550 °C to 750 °C. Characterizations showed that low temperatures synthesizing leas to small diameters and high surface area as well as high porosity. Current density–voltage (J-V) analysis demonstrated that low temperature synthesized samples shows the better performance. Also, EIS measurements showed that series resistance increases as preparation temperature increases; but did not show regular correlation about CTR.

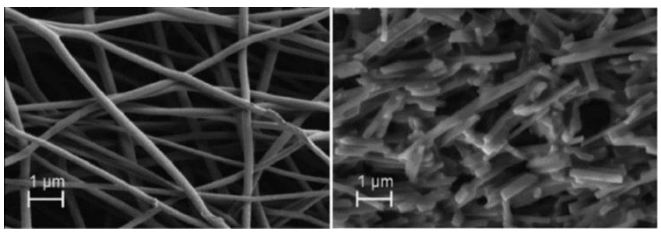

Fig. 5 Top view SEM image of the electro-spun carbon nanofiber (ECN) sheets (left) SEM image of top-view on CE (right)

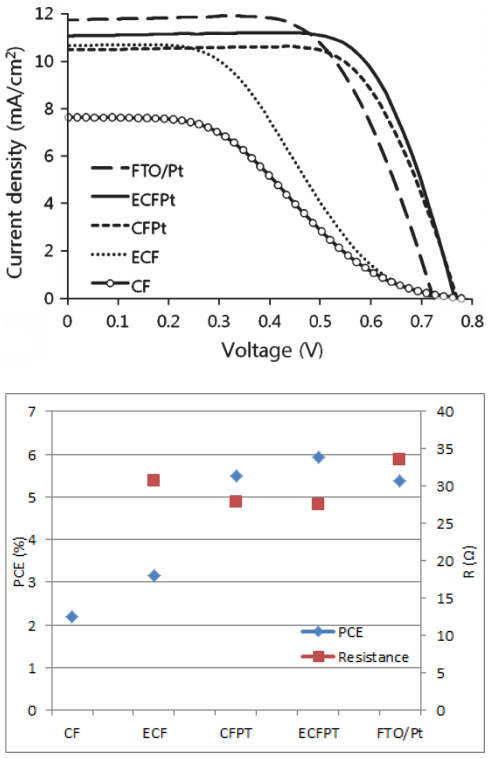

Fig. 6 Photocurrent–voltage curves of DSSC with different counter electrodes (a); PCE and CRT value for samples which get extracted from J-V and EIS measurement (b) [46].

The low temperature samples may satisfy the threshold dimensions. Also, effect of thickness of CEs on cell performance was investigated, in the case of low temperature samples and followed by thickness characterization. The best results both in PCE and series resistance achieved in the case of thick samples. As overall, it can be stated that thicker layer, but small and entire CNFs explain considerable performance through more catalytic sites introduced in the porous media.

4. Porous Carbon Structure

It was assigned that regard to CE porous structures increase the active area; i.e. available sites to redox reaction get raise. Recently, among carbon family, porous carbon has received great attention as CE component.

Mesoporous silica materials (surface area around 1300 m^2/g) [48] are one of the best structures as adsorbent; due to high porosity that it presents. Large porous carbon structures were characterized by nitrogen adsorption isotherm. It was revealed that surface area and porosity were higher than mesoporous silica materials [49]. According to the potential, this high porous media may employ as promise CE, through facile diffusion of electrolyte to redox reactions. Xing et al. [50] made hierarchical types of porous carbon samples (C-1, C-2 and C-3) from rice husk as DSSC CEs. Pre-treatments to prepare samples were included of pre-carbonization (C-1), leaching (C-2) and lastly, activation process of leached samples (C-3). The measurements resulted in significant findings. Pore volume of C-1 was lower compared to C-2, which has been obtained due to inorganic matter leaching from C-1 (mainly silica); also, very lower volume respect to the C-3, which comes from activation of C-2 (pore

opening and widening). Table 3 shows pores specifications of the samples. The DSSCs proposed by all fabricated and reference (Pt) samples as CE. It's clear that C-3 is more capable in catalytic activity rather others. The key point refers to high void volume which has been emerged. CV was studied to investigate the catalytic activity of all samples (Fig. 7).

Table 3 Porous samples characterization

Sample	S_{micro} ($m^2\ g^{-1}$)	S_{meso} ($m^2\ g^{-1}$)	V_{mico} ($cm^3\ g^{-1}$)	V_{meso} ($cm^3\ g^{-1}$)
C-1	247.1	21.6	0.13	0.02
C-2	231.3	89.9	0.11	0.20
C-3	962.4	132.2	0.35	0.26

The peak current densities can be used to evaluate the catalytic activities of the CEs. C-3 possesses the highest current density value which is attributed to high degree of porosity. Hierarchical porous structures have been consisted of large-size mesopores and a large number of micropores; which has stronger catalytic activity. Mesopores can act as transport channels to the micropores for the electrolyte. Both meso- and micropores together provide a criterion for accessible surface area, consequently, electrocatalytic activities enhances. By similar argument, C-1 has the weakest catalytic activity. In other words, the low activity is ascribed to low surface area and limit accessibility of electrolyte to the micropore.

5. Graphene

Tow dimensional structures of the graphite are called graphene which has been engrossed great attentions, recently. It has arrayed sp^2 hybridization of carbon atoms. The layers of one thick atom, possess promise properties such as high mobility carrier (i.e. charge carriers can travel long distances without scattering ~10.000 cm^2/Vs), excellent thermal conductivity, optical transparency, good mechanical resistance and considerable corrosion resistance [51, 52 and 53]. According to such characteristics, graphene has offered great potential to electronic devices like DSSCs. Due to high surface area that presents in the planar structures, it is demonstrated high potential to redox reactions.

Moreover, it has been proved that catalytic activity enhances by introducing oxygen species; also structural defects has the same effect on catalytic activity [54].

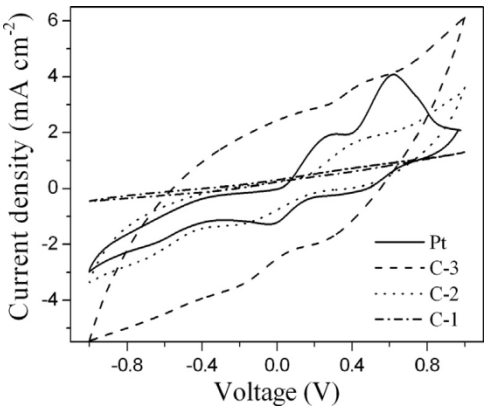

Fig. 7 CV measurement; C-3 shows the intense peak [50].

Oxidative exfoliation of graphite (Hummer) is one of the most conventional methods to produce graphene. Other techniques also are available to provide graphene nanosheets; such as chemical reduction of graphene oxide colloids under microwave radiation, electrophoretic deposition (EPD) which is followed by annealing, etc. However, oxidative exfoliation method to preparation of CE may be defined thermally or chemically. Substantially, thermal exfoliation prepares graphene nanosheets to CE through introducing defect; thereby, it increases surface area. This method is carried out by dispersing graphite in mixed solution of Nafion: Ethanol, and then drop casting on FTO substrate. However, Nafion as a binder is employed to better attachment on the substrate. On the other hand, chemically is not as easily as thermally. The process included oxidative exfoliation by hydrazine reduction which gets maximum efficiency around 6.8%. However annealing treatment is needed as a key step regard to deposition over TCO. Optimized temperature to this process is about 400 ˚C; and above that graphene sheets are peeled-off from substrate. Regardless to additional thermal treatment which could lead to numerous damages over nanosheets, the binding to the TCO could be considerable.

Functional graphene sheets also have been defined as one of the best candidates. The high surface area, structure defects and oxygen-containing group such as hydroxyl, carbonyl and epoxide, have shown promise results to CE operation [55, 56 and 57]. Surface area and structure defects have been discussed before; following, the effect of oxygen-containing groups will be defrayed.

Extremely pure graphene has an excellent conductivity, but possesses limited number of active sites to electrocatalytic mechanisms. Therefore functional groups can be useful to this manner. As far as we know, it is noticeable that, just oxygen-containing group can improve catalytic property [43].

Kavan and Aksay, solely, proved that as oxygen-containing groups increase, catalytic activation strongly gets raise. Since, there is some reverse report such as Jeon's work [58, 59 and 60], it could be concluded that there is an optimum number of oxygen-containing groups to propose promise catalytic activity.

Electrochemical methods have developed to produce graphene oxide sheets. In this regard, after pre-treatment, graphite precursor underwent exfoliation for 4 hr. using dilute H_2SO_4 solution. Then, it was processed to result the slurry. The slurry was doctored blade on clean FTO substrate and followed by drying at 350 °C for 1 hr. Surface morphology of the fabricated CEs showed that exfoliation has peeled off the graphitic structure to pave the way for oxygen entered during oxidation process; thus, it becomes a promise structure to CE. As they expect, J-V characterization of the DSSCs exhibited graphene oxide (GO) with PCE of 0.90% can have excellent performance rather Pt one (reference) with PCE of 0.27% [61]. However, it is more likely to offer higher performance, if it satisfies the optimized value of oxygen matter.

Graphene oxide (GO) was prepared using a modified Hummers method from graphite. It followed by reduction to form reduced-graphene oxide (rGO) by applying a modified photo-thermal reduction process (P-rGO). The samples were employed as CE; also, Pt CE was fabricated as reference [62]. Characterizes include J-V and CV were carried out to compare their performance (Fig 8). Obviously, the P-rGO has offered better performance rather than GO. It has been demonstrated that P-rGO as a CE can achieve 95% of that of Pt-based. Also, CV measurements were studied reduction reactions of the electrodes and revealed that P-rGO electrode shows the highest peak current density value (J=4.70 mA.cm^{-2}). It describes fast kinetics of the redox reactions, compared to the GO and Pt electrodes.

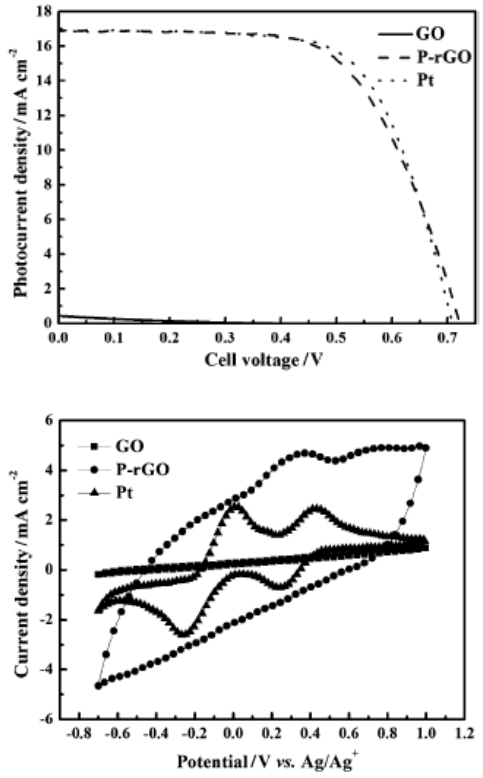

Fig. 8 J–V curves of DSSCs with CEs containing the films of GO, P-rGO, and Pt (top); Cyclic voltammogram of the electrodes with GO, P-rGO, and Pt (bottom) [62].

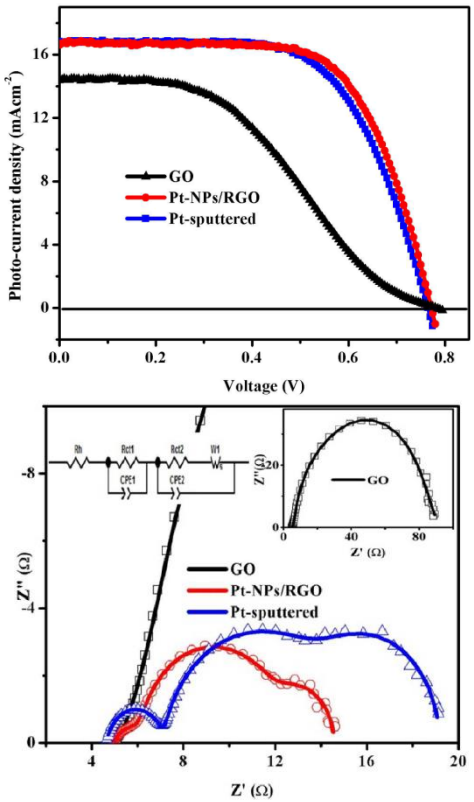

Fig. 9 J-V characteristics of DSSCs (top); EIS characteristic (bottom) for three kind of electrode [65].

Also, EIS measurements exhibited that GO has the highest CTR and series resistance. Hybrid systems received high interest for CE fabrication. Yen et al. [63] introduced Pt nanoparticles on graphene-coated FTO substrate (Pt NPs/GR) as a hybrid CE. In comparison of conventional Pt CE, the measurements showed that the hybrid system demonstrated significant reduction in CTR as well as diffusion resistance (R_d); also, the FF improved. Pt NPs/GR showed PCE of 6.35% higher than that of conventional (5.47%). According to the aforementioned discuss, thermal approach to fabricate the graphene may result in proper condition. Introduction of thermal nanosheets offers high performance.

It was assigned that fabrication procedure can be considered as a key factor on the result performance, directly. Thus, a given materials which are employed in different procedures probably will demonstrate different results. Hybrid Pt/rGO electrode was synthesized by using Pt precursor of H_2PtCl_6 and GO (modified Hummer's method) [64]. To reduce both GO and Pt precursor, synthesize followed with post thermal treatments. The J-V and EIS characterizations defined high electrocatalytic activity in hybrid electrode emerged by 4% growth in PCE, rather conventional Pt. The claim supports by 10% decrease and 4% increase in resistance and fill factor, respectively. In addition 33% scrounge achieved in H_2PtCl_6 rather than conventional electrodes. Recently, the close system has been investigated, in this regard. Dry plasma reduction was used to hybridizing Pt nanoparticle by GO [65]. GO powder in the form of paste was doctored blade over FTO. Then Pt precursor dropped on GO and followed by reduction in Ar atmosphere. Characterizations showed that structural damages have been recovered through chemical bonding between Pt and rGO. Pt sputtered, GO-coated and hybrid electrodes underwent J-V and EIS characterizations which have been shown (Fig. 9). Hybrid electrode shows 4% improvement in PCE rather than conventional Pt-based; moreover the FF revealed the highest value. It is inferred that internal resistance is the minimum, compared to others. EIS measurements showed that in comparison of conventional CE, hybrid electrode has introduced lower CTR. However, from economic viewpoint, hybrid electrodes scrounge in Pt consume. Jang et al. [66] employed GO and Pt nanoparticles as CE. They fabricated GO CE by spin-coating followed by immobilizing Pt nanoparticles via pulse current electro-deposition. This procedure possesses range of advantages such as given (favourable) particle size, density control, and uniform morphology. Uniformly distribution of Pt nanoparticles with average size of ~30 nm, proposed catalytic sites which enhanced electrolyte reduction rate. Measurement exhibits PCE enhancement more than twofold. However, fill factor and current density revealed the highest value for synthesized electrode. CV and EIS confirmed improvement in electrocatalytic activities of these CEs.

The last three studies which have carried out on very close systems, state the synergic effect of hybrid CE. High mobility of graphene-based systems promotes the charge transferring from TCO; however, Pt species, which was distributed over nanosheets, play as hot catalytic sites. Overall, quick charge transfers as well as fast reductions lead to promise performances.

Among other efforts which have developed cost effective approaches, it can be referred to the study of mallam et al. They sprayed Pt NPs on hot substrates. The measurements revealed that PCE enhanced significantly, yet this method results in reduction of Pt consumption by 86%; which leads to cheap DSSCs [67, 68]. In fact, they examined the new procedure for Pt NPs which has been defined as high surface over broad substrate; overall, it resulted in wide distributed of catalytic sites.

Another kind of hybridization which has been introduced in CE was consisted of rGO and ordered mesoporous carbon (OMC). The

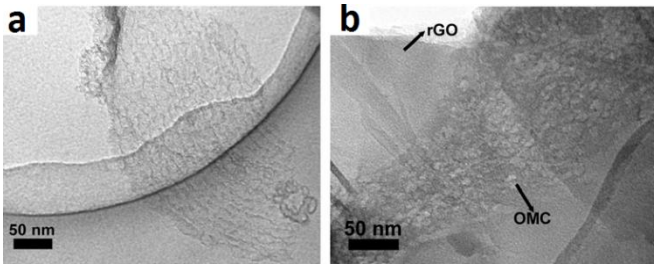

Fig. 10 TEM image of OMC (a); rGO-OMC composite (b) [69].

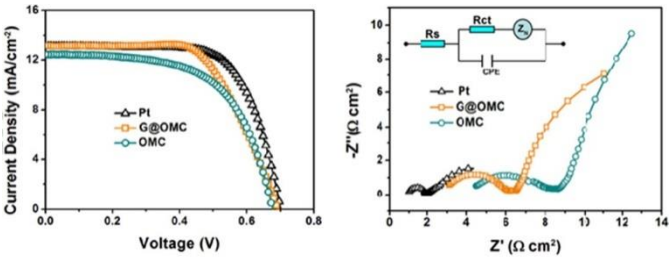

Fig. 11 J-V (left) and EIS characteristics (right) of DSSCs with different CEs [69].

composite was prepared by Tang et al. method. Measurements indicated that the primary particles of the OMC result in well-interconnected by the graphene networks (Fig. 10). Also N_2 isotherm confirmed that ordered mesoporous structures have been retained on both OMC and rGO/OMC without any deformation. It was demonstrated that volume and size of the pores show the increase of 17% and 41% in rGO-OMC, respectively, rather OMC; also, resistance 65% decreased. rGO/OMC, OMC, and Pt were employed as CE in DSSCs. It is expected that increased porosity in rGO/OMC leads to higher surface area to reactions, thereby facile diffusion for electrolyte. With this in mind, synergy effects may define the rGO/OMC as competitive alternative for Pt-based. However, it was inferred from J-V characterize (Fig. 11). Photovoltaic parameters proved that PCE and FF in hybrid electrode can achieve ~90% of those of Pt-based. Also, EIS (Fig. 11) parameters of conventional Pt electrode were evaluated about one third of hybrid one. These findings showed potential of new hybrid electrode to efficient DSSCs [69]. Indeed, the combination of high charge mobility in graphene with the catalytic activity of OMC, which could be deduced from Fig. 11 (left), avoids from several recombinations and demonstrates high performance for composite electrode through higher photocurrent.

6. Carbon Nanotube

CNTs like other members of carbon family, which were reviewed, offer good properties such as high electrical conductivity, high structural porosity, etc. Amongst, Multi Wall Carbon Nanotube (MWCNTs) is an alternative material to CE; it is referred to the active area which offers by several walls. MWCNTs were grown by chemical vapor deposition at low temperature of 530°C; using ammonia and acetylene gas as precursor. Pt as reference and MWCNT CEs were synthesized in similar procedure. Linear resistance was measured by using tow probes and was found that CEs electrical resistance is emerged as low as comparable. Also, I-V characterization revealed that MWCNT electrode results in 16% enhancement in PCE, rather reference one (Fig. 12). Also, J_{sc}, V_{oc} and FF increased 18%, 10% and 22%, respectively [70]. The improvement states high potential in catalytic activity which arises from broad inner and outer surface area. From other studies which

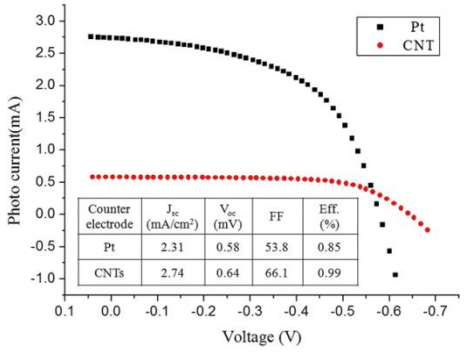

Fig. 12 I-V curve characteristics of DSSCs with different counter electrodes [70].

have focused on MWCNTs, it can be referred to study of Bae group. They investigated on three different structures of MWCNTs (raw, purified, and purified & ground). Purified & ground MWCNT CE showed an overall photovoltaic efficiency of 4.94%; which satisfied 97% of conventional Pt electrodes performance [71]. Also, a number of researches was proposed based on Pt composite of CNTs and exhibited remarkable results. Huang et al. synthesized Pt NPs/MWCNTs composite and treated by imide functionalized materials. The composition was spin-coated as CE, subsequently. The measurements exhibited high catalytic activity which can be attributed to broad surface area which had been prepared through composite structure; also PCE of around 8% and high current density were ascribed to well-done redox species (I3-) reduction.

Recently, sedghi et al. [72] has compared three different CE; Pt-based, MWCNTs-based, and hybridized Pt/MWCNTs. Pt electrode was prepared by immersing FTO on H_2PtCl_6 solution and followed by thermal treatment; MWCNTs- and Pt/MWCNTs-CEs both were fabricated by spraying MWCNTs solution and Pt-loaded MWCNTs solution on FTO; and thermal treatment, finally. Morphology characterization showed that first sample (Pt) has discontinuity of coverage on FTO substrate. However, it revealed large pores on Pt film, thus catalytic active area is not considerable. Second sample (MWCNTs) showed uniform layer with less porosity. Also, interesting result obtained in the case of Pt/MWCNTs electrode, it was revealed that large pores on Pt film has enfolded nanotubes and hence enhances catalytic active area. Therefore, PCE of the DSSCs which were proposed, expected to be in order of Pt/MWCNTs > Pt > MWCNTs. Also, the highest current density peak in CV measurements, which belongs to hybrid electrode, revealed that Pt/MWCNTs have the highest kinetic rate of reduction.

Further systems in hybridization modes were constructed [73]. MWCNTs, Graphene (GR), graphene/MWCNTs (GC) hybrid in different ratio of components and Pt as reference were introduced as CEs. Hybrid types were consisted of two ratios in composition: 30 wt% graphene (70 wt% MWCNT) and 70 wt% graphene (30 wt% MWCNT) which notify as GC37 and GC73, respectively. Fabrication of carbonaceous CEs was the same and included mixing by other components and ultrasonic treatment to result in paste. Subsequently, resulted paste underwent solvent-casting over FTO under vacuum. DSSCs were introduced by each sample and were characterized by J-V; rounded values have stood in the Table 4.

FF in all carbonaceous electrodes shows reduction rather than conventional Pt electrode. Compared to the MWCNTs, GR possesses higher contact area. On the other hand, it possesses higher diffusion resistance and isolated aromatic tails; which comes from its synthesis procedure and leads to lower FF. Also, higher current density, in the case of GR, is satisfied through the broad surface area as well as more surface defects. Hybrid electrode

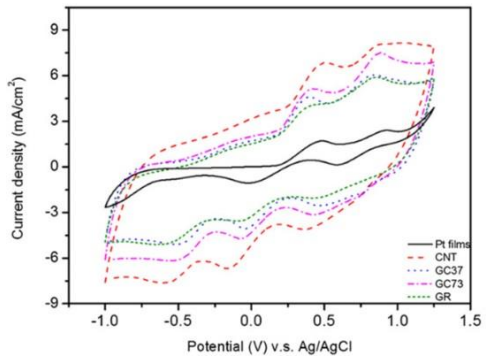

Fig. 13 CV measurement; at a scan rate of 50 mV s^{-1} [73].

Table 4 Current-Voltage characterization

Electrode	J_{sc} (mA cm^{-2})	V_{oc} (V)	FF (%)	PCE (%)
Platinum films	10.26	0.72	0.70	5.09
GR	11.95	0.78	0.42	3.90
GC37	11.52	0.74	0.47	3.94
GC73	11.42	0.77	0.53	4.66
CNT	9.12	0.77	0.53	3.73

resulted in considerable performance, because of interconnections between isolated aromatic domains. Also, the processed network reduces diffusivity resistance of the electrolyte. G73 was defined better performance than G37; the main reason is defined by MWCNTs aggregation which makes high diffusion resistance. Moreover, CV measurement was done (Fig. 13).

MWCNTs have demonstrated strong effect; as a matter of fact the wide specific surface area leads to improvement of active sites reaction through strong π-π Interactions. Although, the MWCNTs show the highest current density, but the electron transfer rate is poor, compared to the other samples (GR and GC hybrid). As overall, GC73 offers best results to replace conventional Pt CEs. It benefits from active sites reaction (which are imposed by MWCNTs), high electron transferring and also surface defects (which come from GR). However, electron mobility plays greater role in this regard; that's why GC73 leads to better performance.

IV. Carbonaceous Derivatives

Recently, manipulations of materials and methods have been resulted in novel carbonaceous nanomaterials-based CEs. These approaches mainly included functionalized, composed, and doped carbon structures. Here, we proceed in some important ones.

1. Composed carbonaceous electrode

a) Carbon based electrode

Recently, polymer hybrid of carbon black was examined as CE [74]. Poly(3,4-ethylenedioxythiophene) : polystyrenesulfonate/carbon (PEDOT:PSS/C) was employed as CE in DSSC. The conductive polymer may improve the charge transfer and enhance the performance. However, the characterizations resulted in this manner, properly. The measurements demonstrated that the reduction in CTR is recognizable and the catalytic activity has increased, clearly.

Also, inorganic material was employed as a candidate for CE by Mingxing et al. [75]; they reported considerable results in the regard of fabricated Ni_5P_4/C, Ni_5P_4 and MoP, as CEs and was compared to that of conventional Pt. The J-V and EIS) results have stood in the Table 5.

Table 5 CTR and PCE for various CE composition

Electrode	CTR (Ω cm^2)	PCE (%)
MoP	27.4	4.92
Ni_5P_4	18.9	5.71
Ni_5P_4/C	2.2	7.54
Pt	3	7.76

Clearly, the MoP and Ni_5P_4 CEs cannot be as competitive to the conventional Pt. low PCE are directly attributed to the high CTR. When Ni_5P_4 incorporated to the carbonaceous porous media, the CTR decreased significantly, even lower than that of Pt; which states high catalytic activity of carbon porous substrate. The slightly differential of PCE for carbonaceous and conventional may come from hybrid mismatching of Ni_5P_4/C composition.

Gentian et al. [76] fabricated a CE based high porous molybdenum sulfide–carbon (MoS_2–C) hybrid film using in situ hydrothermal method. The measurements of proposed DSSC indicated better performance, compared to Pt and MoS_2–C reference ones. CV analysis (Fig. 14) revealed that MoS_2–C possesses highest current density in both reduction and oxidation peaks which ascribed to the lowest CRT on the electrolyte–electrode interface. This translates high electrocatalytic activity and rate reduction for electrolyte in comparison of others. They progressed the study by investigation of carbon content of successful electrode and concluded that there is an optimum value for composited electrode. It may be related to the defects which emerge in various hybrid ratios.

b) Graphene based electrode

As it was assigned frequently, electrochemical activity, conductivity as well as cost contribute in DSSCs performance. Recently, polymerization of carbon-based material has emerged as potential CEs for these devices. Gentian et al. [77] electrodeposited the composite of graphene/PEDOT:PSS over FTO substrate by employing electrochemical polymerization method. The DSSCs were proposed based on various fraction of graphene in hybrid system CEs, as well as reference Pt one. Measurements were done and results have summarized in Table 6.

Table 6 CTR and PCE for various CE compositions

Electrode	CTR (Ω cm^2)	PCE (%)
0.01 wt.%	6.22	6.33
0.03 wt.%	4.37	6.96
0.05 wt.%	2.74	7.86
0.10 wt.%	3.62	7.10
0.15 wt.%	5.68	6.58
Pt	2.82	7.31

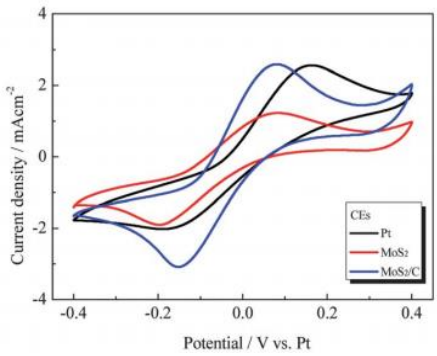

Fig. 14 CV measurements for fabricated and conventional CEs [77]

Clearly, 0.05 wt.% is an optimum ratio of graphene incorporated composition. The significantly enhancement of the performance for optimum DSSC may be due to the large active surface-area, lower surface resistivity and the higher electrical conductivity of the graphene flake and PEDOT:PSS synergistic catalytic effect, which is advantageous to increase the redox reaction rate on the CE side.

c) Carbon Nanotube based electrode

In this regard, conductive polymers such as polyaniline has been employed in DSSCs and presented efficient performance. Xiao et al. [78] fabricated the cobalt sulfide ($CoS_{1.097}$) nanoclusters/MWCNT nanocomposites embedded polyaniline (PANI) film (PANI/MWCNT@$CoS_{1.097}$) (Fig. 15) CE and compared with Pt reference one. The J-V measurements revealed that composite electrode can obtain the PCE of 98% of conventional Pt. the improvement of conversion efficiency is attributed to the numerous interconnects between the highly intrinsic electrocatalytic MWCNT@$CoS_{1.097}$ nanocomposites through polymer matrix. In fact, the insertion of nanocomposites into the conductive lamellas has introduced many reduction centers to oxidized electrolyte.

However, it was proved that the same composition of CNT@$CoS_{1.097}$ potentially can results in promise DSSC [79]. The PCE of non-polymerized composed electrode which was fabricated by spray coating followed by annealing under the N_2 atmosphere. X-ray diffraction characterization revealed that the crystalline $CoS_{1.097}$ has transferred to the form of Co_9S_8 which possesses higher electrochemical activity. Also, the measurement defined reduction of 23 and 28% in CTR compared to the initial form ($CoS_{1.097}$) and Pt

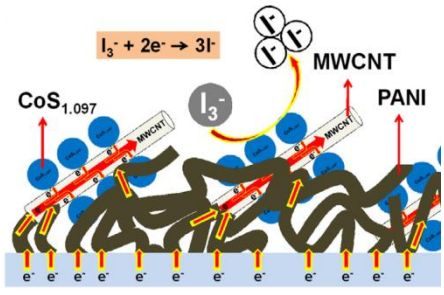

Fig. 15 Schematic of composite electrode

sputtered. Conclusively, the composed electrode resulted in 6 and 4% improvement in PCE rather initial and Pt CEs.

2. Doped carbonaceous electrode

Recently, employing doped carbon nanostructures as CE have been defined as an interesting topic for DSSCs. Scientists have worked on the improvement of electrocatalytic performance for carbonaceous nanostructures, especially through heteroatom doping. Generally, there are two main effects which simulate the potential of doped systems: (1) the conjugation effect of the lone pair electrons on the heteroatoms and carbonaceous π-system may reduce the barrier to I_3^- reduction; (2) the doped heteroatoms are usually located at edge or defects sites, which are chemically active, thereby cause acceleration redox reactions.

a) Graphene based electrode

In this regard, Peng et al. [80] have proposed DSSC based microwave exfoliated graphene (MEG) and nitrogen doped one (N-MEG) as a Pt-free CE. The FESEM images of fabricated electrode for both samples have been shown in Fig. 16. As images illustrate, it is defined high degree of porosity in the N-MEG sample. Also, it was demonstrated that CTR is correlated inversely to the available surface area, in the case of carbon nanostructure. Consequently, broad surface area, in the case of N-MEG leads to lower CTR, compared to MEG electrode. Moreover the samples underwent EIS characterizations. As expected, it revealed the CTR of 6.13 and 1.31 Ω for MEG and N-MEG, respectively. In comparison of conventional Pt electrode, N-MEG introduces more than two times higher resistance.

It could be ascribed to the low charge transfer rate constant of electrolyte for redox reaction due to its relative large peak-to-peak separation.

Further close research proposed nitrogen doped graphene nanoribbons (N-GNR) with the thickness of 7 and 19 μm (N-GNR-1 and N-GNR-3, respectively) and the electrolyte of tiolate/disulphide [81]. The PCE for N-GNR-1 and N-GNR-3 was 3.82% and 5.07% respectively, while reference Pt one resulted in 3.09%. It explains that the carbon based material could lead to superior performance; however, the difference is attributed to the operation of CEs. In this

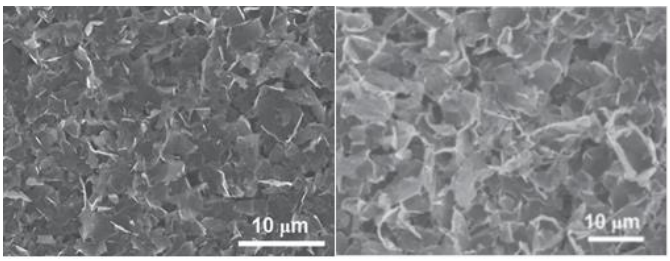

Fig. 16 FESEM images of MEG (left) and N-MEG (right) [80]

regard, IES measurements was done; the CTR value obtained in the order of Pt >> N-GNR-3 > N-GNR-1. However, this is in the counter point of Peng group [80] study and the inconsistency in CTR trends could be explained through deposition thickness; i.e. the deposition thickness is a decisive factor in charge transfer; as far as it can satisfy the charge transfer constant.

Also, phosphor as a dopant was introduced to the reduced graphen oxide (PrGO) and proposed as CE [82]. The performance and the CTR improved rather conventional Pt electrode. The improvement is attributed to conjugation systems over carbon substrates which was defined through phosphorous doing and preparation more active sites.

b) Carbon nanotube based electrode

Yedi et al. [83] examined nitrogen doped carbon nanotube decorated with Co and Ni nanoparticles (NCNT-Co and NCNT-Ni) as CEs. In comparison of Pt-based electrode as reference one (PCE=7.67%), the NCNT-Ni (PCE=8.39%) and the NCNT-Co can achieved the higher conversion efficiency (PCE of 7.75%). The high performance of the fabricated systems is attributed to the high conductivity of CNT rather Pt, higher electrocatalytic activity of nitrogen induced species, and fast reduction of electrolyte which arise from metal nanoparticles. CNT doped electrode like graphene and other porous media, demonstrates higher catalytic activity due to facile permeation of liquid electrolyte, inherently; while non-rough sputter Pt electrode does not offer such a choice.

Conclusions

The efficiency of DSSCs is looking forward to commercialization approach. The present review enfolded a large number of carbonaceous materials as CEs in DSSCs. An ideal CE should propose (a) perfect stability, (b) high catalytic activity and (c) low charge transfer resistance. Platinum as conventional and efficient element in DSSCs CE, faces to several issues such as corrosion, high cost etc. This, conducted the scientists efforts to find an inexpensive alternative and yet with the same performance. As it was reviewed, the carbonaceous matters such as carbon black, nanofiber, graphene, nanotube, have proposed as good a candidate to replace in conventional CEs due to plasticity, simple fabrication procedures and excellent electrochemical activity towards the redox species. The advantages are defined through higher surface area which has been emerged in planar or tubular nanostructure; also, potential electrochemical activity. Moreover, from viewpoint of economic, cost effective carbon electrodes have been emerged considerable. However, most of the DSSCs performance, which proposed by carbonaceous CE, is slightly lower than that of fabricated using Pt CE. This mostly comes from various resistances associated to the structurally complex carbon electrodes; such as bulk resistance through the comparatively thick carbon CE, contact resistance to the TCO substrate, the diffusion resistance in the pores of the CE, etc. Despite the problems, carbonaceous CEs still offer distinct advantages of low cost and long-term stability which can reveal DSSCs potential among various photovoltaic devices. Thus, the study of new organic and inorganic compounds as an alternative material to Pt in DSSCs is a promising research area which is essential to reduce the cost of the devices for commercialization.

Notes and references

1. A. Herzog, T. Lipman and D. Kammen, Renewable Energy Sources. Our Fragile World: Challenges and Opportunities for Sustainable Development, Forerunner to the Encyclopedia of Life Support Systems (EOLSS), vol. 1, Section 1. UNESCO-EOLSS Secretariat, EOLSS Publishers Co. Ltd, (2001).
2. J. Nelson, *The physics of solar cells*. World Scientific, (2003).
3. I. Müller, A history of thermodynamics: the doctrine of energy and entropy. Springer Science & Business Media, (2007).
4. Y. Xie, P. Joshi, S. B. Darling, Q. Chen, T. Zhang, D. Galipeau and Q. Qiao, The Journal of Physical Chemistry C **114** (41), 17880 (2010).
5. X. Wang, S. Karanjit, L. Zhang, H. Fong, Q. Qiao and Z. Zhu, Applied Physics Letters **98** (8), 082114 (2011).
6. P. Joshi, Z. Zhou, P. Poudel, A. Thapa, X.-F. Wu and Q. Qiao, Nanoscale **4** (18), 5659 (2012).
7. P. Poudel, L. Zhang, P. Joshi, S. Venkatesan, H. Fong and Q. Qiao, Nanoscale **4** (15), 4726 (2012).
8. P. Poudel, A. Thapa, H. Elbohy and Q. Qiao, "Improved performance of dye solar cells using nanocarbon as support for platinum nanoparticles in counter electrode", Nano Energy **5**, 116 (2014).
9. Z. A. Krasnaya, V. V. Kachala and S. G. Zlotin, Mendeleev Communications **24** (6), 377 (2014).
10. B. Liu, Y. Sun, X. Wang, L. Zhang, D. Wang, Z. Fu, Y. Lin and T. Xie, Journal of Materials Chemistry A, (2015).
11. B. O'regan and M. Grfitzeli, nature **353**, 24 (1991).
12. M. Zalas, B. Gierczyk, M. Klein, K. Siuzdak, T. Pędziński and T. Łuczak, Polyhedron **67**, 381 (2014).
13. Y.-G. Kim, C.-H. Shim, D.-H. Kim, H. J. Lee and H.-J. Lee, Thin Solid Films **520** (6), 2257 (2012).
14. D. Susanti, M. Nafi, H. Purwaningsih, R. Fajarin and G. E. Kusuma, Procedia Chemistry **9**, 3 (2014).
15. D.-J. Yun, J. Kim, J. Chung, S. Park, W. Baek, Y. Kim, S. Kim, Y.-N. Kwon, J. Chung and Y. Kyoung, Journal of Power Sources **268**, 25 (2014).
16. J. Nelson and R. E. Chandler, Coordination Chemistry Reviews **248** (13), 1181 (2004).
17. H. M. Upadhyaya, S. Senthilarasu, M.-H. Hsu and D. K. Kumar, Solar Energy Materials and Solar Cells **119**, 291 (2013).
18. J. Wu and Z. M. Wang, *Quantum Dot Solar Cells*. Springer, (2014).
19. H. Ma, J. Tian, S. Bai, X. Liu and Z. Shan, Electrochimica Acta **137**, 138 (2014).
20. J. Jin, X. Zhang and T. He, "Self-Assembled CoS_2 Nanocrystal Film as an Efficient Counter Electrode for Dye-Sensitized Solar Cells", Journal of Physical Chemistry C **118** (43), 24877 (2014).
21. H. Hoshi, S. Tanaka and T. Miyoshi, "Pt-graphene electrodes for dye-sensitized solar cells", Materials Science and Engineering: B **190**, 47 (2014).

22. T.-T. Duong, T. Q. Tuan, D. V. A. Dung, N. Van Quy, D.-L. Vu, M. H. Nam, N. D. Chien, S.-G. Yoon and A.-T. Le, "Application of polyaniline nanowires electrodeposited on the FTO glass substrate as a counter electrode for low-cost dye-sensitized solar cells", Current Applied Physics **14** (12), 1607 (2014).
23. G. Wang, S. Kuang, D. Wang and S. Zhuo, "Nitrogen-doped mesoporous carbon as low-cost counter electrode for high-efficiency dye-sensitized solar cells", Electrochimica Acta **113**, 346 (2013).
24. G. Dutta, A.-M. J. Haque and H. Yang, "Improvement of the electrocatalytic activities of long-aged Pt electrodes and the change of the improved activities with aging", Electrochimica Acta **141**, 319 (2014).
25. C.-H. Tsai, C.-H. Chen, Y.-C. Hsiao and P.-Y. Chuang, "Investigation of graphene nanosheets as counter electrodes for efficient dye-sensitized solar cells", Organic Electronics **17**, 57 (2015).
26. V.-D. Dao, S.-H. Kim, H.-S. Choi, J.-H. Kim, H.-O. Park and J.-K. Lee, "Efficiency Enhancement of Dye-Sensitized Solar Cell Using Pt Hollow Sphere Counter Electrode", Journal of Physical Chemistry C **115** (51), 25529 (2011).
27. V.-D. Dao and H.-S. Choi, "An Optimum Morphology of Platinum Nanoparticles with Excellent Electrocatalytic Activity for a Highly Efficient Dye-Sensitized Solar Cell", Electrochimica Acta **93**, 287 (2013).
28. C.-C. Yang, H. Q. Zhang and Y. R. Zheng, "DSSC with a novel Pt counter electrodes using pulsed electroplating techniques", Current Applied Physics **11** (1), S147 (2011).
29. J. Wu, Z. Tang, Y. Huang, M. Huang, H. Yu and J. Lin, "A dye-sensitized solar cell based on platinum nanotube counter electrode with efficiency of 9.05%", Journal of Power Sources **257**, 84 (2014).
30. C. Zhao, Y. Shi, Z. Zhong and T. Ma, "Screen-printed Pt counter electrodes exhibiting high catalytic activity", Chinese Journal of Catalysis **35** (2), 219 (2014).
31. F. Miao, B. Tao and P. K. Chu, "Enhancement of the efficiency of dye-sensitized solar cells with highly ordered Pt-decorated nanostructured silicon nanowires based counter electrodes", Electrochimica Acta **96**, 61 (2013).
32. C. Bao, H. Huang, J. Yang, H. Gao, T. Yu, J. Liu, Y. Zhou, Z. Li and Z. Zou, "The Maximum Limiting Performance Improved Counter Electrode Based on a Porous Fluorine Doped Tin Oxide Conductive Framework for Dye-Sensitized Solar Cells", Nanoscale **5** (11), 4951 (2013).
33. Y. Gong, C. Li, X. Huang, Y. Luo, D. Li, Q. Meng and B. B. Iversen, "Simple Method for Manufacturing Pt Counter Electrodes on Conductive Plastic Substrates for Dye-Sensitized Solar Cells", ACS applied materials & interfaces **5** (3), 795 (2013).
34. K. Aitola, J. Halme, N. Halonen, A. Kaskela, M. Toivola, A. G. Nasibulin, K. Kordás, G. Tóth, E. I. Kauppinen and P. D. Lund, "Comparison of dye solar cell counter electrodes based on different carbon nanostructures", Thin Solid Films **519** (22), 8125 (2011).
35. S. Xu, Y. Luo and W. Zhong, "Investigation of catalytic activity of glassy carbon with controlled crystallinity for counter electrode in dye-sensitized solar cells", Solar Energy **85** (11), 2826 (2011).
36. C.-D. Wu, T.-H. Fang and J.-Y. Lo, "Effects of pressure, temperature, and geometric structure of pillared graphene on hydrogen storage capacity", international journal of hydrogen energy **37** (19), 14211 (2012).
37. H. Idriss and M. A. Barteau, "Active sites on oxides: From single crystals to catalysts", Advances in Catalysis **45**, 261 (2000).
38. K. Imoto, K. Takahashi, T. Yamaguchi, T. Komura, J.-i. Nakamura and K. Murata, "High-performance carbon counter electrode for dye-sensitized solar cells", Solar Energy Materials and Solar Cells **79**,459 (2003).
39. T. N. Murakami, S. Ito, Q. Wang, M. K. Nazeeruddin, T. Bessho, I. Cesar, P. Liska, R. Humphry-Baker, P. Comte and P. Péchy, "Highly Efficient Dye-Sensitized Solar Cells Based on Carbon Black Counter Electrodes", Journal of the Electrochemical Society **153** (12), A2255 (2006).
40. G. Veerappan, K. Bojan and S.-W. Rhee, "Amorphous carbon as a flexible counter electrode for low cost and efficient dye sensitized solar cell", Renewable Energy **41**, 383 (2012).
41. J. Balamurugan, R. Thangamuthu, A. Pandurangan and M. Jayachandran, "Facile fabrication of dye-sensitized solar cells utilizing carbon nanotubes grown over 2D hexagonal bimetallic ordered mesoporous materials", Journal of Power Sources **225**, 364 (2013).
42. P. Joshi, Y. Xie, M. Ropp, D. Galipeau, S. Bailey and Q. Qiao, "Dye-sensitized solar cells based on low cost nanoscale carbon/TiO_2 composite counter electrode", Energy & Environmental Science **2** (4), 426 (2009).
43. P. Poudel and Q. Qiao, "Carbon nanostructure counter electrodes for low cost and stable dye-sensitized solar cells", Nano Energy **4**, 157 (2014).
44. J. Z. Chen, Y. C. Yan and K. J. Lin, "Effects of Carbon Nanotubes on Dye-Sensitized Solar Cells", Journal of the Chinese Chemical Society **57** (5B), 1180 (2010).
45. P. Joshi, L. Zhang, Q. Chen, D. Galipeau, H. Fong and Q. Qiao, "Electrospun Carbon Nanofibers as Low-Cost Counter Electrode for Dye-Sensitized Solar Cells", ACS applied materials & interfaces **2** (12), 3572 (2010).
46. H. Pak and Y. R. Yoo, "Surface Treatment Effect of Carbon Fiber Fabric Counter Electrode in Dye Sensitized Solar Cell", Journal of nanoscience and nanotechnology **12** (2), 1679 (2012).
47. D. Sebastián, V. Baglio, M. Girolamo, R. Moliner, M. Lazaro and A. Arico, "Carbon nanofiber-based counter electrodes for low cost dye-sensitized solar cells", Journal of Power Sources **250**, 242 (2014).
48. H. Nagata, M. Takimura, Y. Yamasaki and A. Nakahira, "Syntheses and Characterization of Bulky Mesoporous Silica MCM-41 by Hydrothermal Hot-Pressing Method", Materials transactions **47** (8), 2103 (2006).

49. S. Thomas, T. Deepak, G. Anjusree, T. Arun, S. V. Nair and A. S. Nair, "A review on counter electrode materials in dye-sensitized solar cells", Journal of Materials Chemistry A **2** (13), 4474 (2014).
50. G. Wang, D. Wang, S. Kuang, W. Xing and S. Zhuo, "Hierarchical porous carbon derived from rice husk as a low-cost counter electrode of dye-sensitized solar cells", Renewable Energy **63**, 708 (2014).
51. H. Y. Mao, Y. H. Lu, J. D. Lin, S. Zhong, A. T. S. Wee and W. Chen, "Manipulating the electronic and chemical properties of graphene via molecular functionalization", Progress in Surface Science **88** (2), 132 (2013).
52. D. Das and H. Rahaman, Carbon Nanotube and Graphene Nanoribbon Interconnects. Crc Press, (2014).
53. T. Dürkop, S. Getty, E. Cobas and M. Fuhrer, "Extraordinary mobility in semiconducting carbon nanotubes"; Nano letters **4** (1), 35 (2004).
54. Z. Lu, G. Xu, C. He, T. Wang, L. Yang, Z. Yang and D. Ma, "Novel catalytic activity for oxygen reduction reaction on MnN4 embedded graphene: A dispersion-corrected density functional theory study", Carbon **84**, 500 (2015).
55. T. F. Chung, T. Shen, H. Cao, L. A. Jauregui, W. Wu, Q. Yu, D. Newell and Y. P. Chen, "Synthetic Graphene Grown by Chemical Vapor Deposition on Copper Foils", International Journal of Modern Physics B **27** (10), (2013).
56. V.-D. Dao, L. L. Larina, H. Suh, K. Hong, J.-K. Lee and H.-S. Choi, "Optimum strategy for designing a graphene-based counter electrode for dye-sensitized solar cells", Carbon **77**, 980 (2014).
57. J. Zhao, L. Liu and F. Li, *Graphene Oxide: Physics and Applications*. Springer, (2014).
58. L. Kavan, J. H. Yum and M. Grätzel, "Optically Transparent Cathode for Dye-Sensitized Solar Cells Based on Graphene Nanoplatelets", ACS Nano **5** (1), 165 (2010).
59. J. D. Roy-Mayhew, D. J. Bozym, C. Punckt and I. A. Aksay, "Functionalized Graphene as a Catalytic Counter Electrode in Dye-Sensitized Solar Cells", ACS Nano **4** (10), 6203 (2010).
60. H. Choi, H. Kim, S. Hwang, Y. Han and M. Jeon, "Graphene Counter Electrodes for Dye-Sensitized Solar Cells Prepared by Electrophoretic Deposition", Journal of Materials Chemistry **21** (21), 7548 (2011).
61. P. K. Singh, U. Singh, B. Bhattacharya and H.-W. Rhee, "Electrochemical synthesis of graphene oxide and its application as counter electrode in dye sensitized solar cell", Journal of Renewable and Sustainable Energy **6** (1), 013125 (2014).
62. M. H. Yeh, L. Y. Lin, L. Y. Chang, Y. A. Leu, W. Y. Cheng, J. J. Lin and K. C. Ho, "Dye-Sensitized Solar Cells with Reduced Graphene Oxide as the Counter Electrode Prepared by a Green Photothermal Reduction Process", ChemPhysChem **15** (6), 1175 (2014).
63. C. Xu, X. Wang and J. Zhu, "Graphene−Metal Particle Nanocomposites", Journal of Physical Chemistry C **112** (50), 19841 (2008).
64. H. H. Gong, S. H. Park, S.-S. Lee and S. C. Hong, "Facile and Scalable Fabrication of Transparent and High Performance Pt/Reduced Graphene Oxide Hybrid Counter Electrode for Dye-Sensitized Solar Cells", International journal of precision engineering and manufacturing **15** (6), 1193 (2014).
65. V.-D. Dao, N. T. Q. Hoa, L. L. Larina, J.-K. Lee and H.-S. Choi, "Graphene–platinum nanohybrid as a robust and low-cost counter electrode for dye-sensitized solar cells", Nanoscale **5** (24), 12237 (2013).
66. H.-S. Jang, J.-M. Yun, D.-Y. Kim, S.-I. Na and S.-S. Kim, "Transparent graphene oxide–Pt composite counter electrode fabricated by pulse current electrodeposition-for dye-sensitized solar cells", Surface and Coatings Technology **242**, 8 (2014).
67. A. Iefanova, J. Nepal, P. Poudel, D. Davoux, U. Gautam, V. Mallam, Q. Qiao, B. Logue and M. F. Baroughi, "Transparent platinum counter electrode for efficient semi-transparent dye-sensitized solar cells", Thin Solid Films **562**, 578 (2014).
68. K.-M. Lee, L.-C. Lin, C.-Y. Chen, V. Suryanarayanan and C.-G. Wu, "Preparation of high transmittance platinum counter electrode at an ambient temperature for flexible dye-sensitized solar cells", Electrochimica Acta **135**, 578 (2014).
69. W. Sun, T. Peng, Y. Liu, N. Huang, S. Guo and X. Zhao, "Ordered mesoporous carbon decorated reduced graphene oxide as efficient counter electrodes for dye-sensitized solar cells", Carbon **77**, 18 (2014).
70. J. Y. Roh, Y. H. Kim and C. S. Lee, "Synthesis of MWNTs using thermal chemical vapor deposition for the application of a counter electrode for DSSCs", Current Applied Physics **11** (4), S69 (2011).
71. B. Munkhbayar, S. Hwang, J. Kim, K. Bae, M. Ji, H. Chung and H. Jeong, "Photovoltaic performance of dye-sensitized solar cells with various MWCNT counter electrode structures produced by different coating methods", Electrochimica Acta **80**, 100 (2012).
72. A. Sedghi and H. N. Miankushki, "Effect of Multi Walled Carbon Nanotubes as Counter Electrode on Dye Sensitized Solar Cells", International Journal of Electrochemical Science **9** (4), 2029 (2014).
73. L.-H. Chang, C.-K. Hsieh, M.-C. Hsiao, J.-C. Chiang, P.-I. Liu, K.-K. Ho, C.-C. M. Ma, M.-Y. Yen, M.-C. Tsai and C.-H. Tsai, "A graphene-multi-walled carbon nanotube hybrid supported on fluorinated tin oxide as a counter electrode of dye-sensitized solar cells", Journal of Power Sources **222**, 518 (2013).
74. Gentian Yue, Jihuai Wu' Yaoming Xiao, Jianming Lin, Miaoliang Huang; "Low cost poly(3,4-ethylenedioxythiophene):polystyrenesulfonate/ carbon black counter electrode for dye-sensitized solar cells"; Electrochimica Acta, **67**, 113 (2012).
75. Mingxing Wu, Jin Bai, Yudi Wang, Anjie Wang, Xiao Lin, Liang Wang, Yihua Shen, Zeqing Wang, Anders Hagfeldt and Tingli Ma; " High-performance phosphide/carbon counter electrode for both iodide and organic redox couples in dye-sensitized solar cells"; J. Mater. Chem., **22**, 11121 (2012).

76. Gentian Yue, Jihuai Wu, Yaoming Xiao, Miaoliang Huang, Jianming Lin, and Jeng-Yu Lin; "High performance platinum-free counter electrode of molybdenum sulfide–carbon used in dye-sensitized solar cells"; J. Mater. Chem. A, **1**, 1495 (2013).
77. Gentian Yue, Jihuai Wu, Yaoming Xiao, Jianming Lin, Miaoliang Huang, Zhang Lan, Leqing Fan; "Functionalized graphene/poly(3,4-ethylenedioxythiophene): polystyrenesulfonate as counter electrode catalyst for dye-sensitized solar cells"; Energy **54**, 315 (2013).
78. Yaoming Xiao, Wei-Yan Wang, Shu-Wei Chou, Tsung-Wu Lin, Jeng-Yu Lin; "In situ electropolymerization of polyaniline/cobalt sulfide decorated carbon nanotube composite catalyst toward triiodide reduction in dye-sensitized solar cells"; Journal of Power Sources, **266**, 448 (2014).
79. Sheng-Yen Tai, Man-Ning Lu, Hsin-Ping Ho, Yaoming Xiao, Jeng-Yu Lin; "Investigation of carbon nanotubes decorated with cobalt sulfides of different phases as nanocomposite catalysts in dye-sensitized solar cells"; Electrochimica Acta, **143**, 216 (2014).
80. Peng Zhai, Tzu-Chien Wei, Ya-Huei Chang, Yu-Ting Huang, Wei-Ting Yeh, Haijun Su, and Shien-Ping Feng, "High Electrocatalytic and Wettable Nitrogen-Doped Microwave-Exfoliated Graphene Nanosheets as Counter Electrode for Dye-Sensitized Solar Cells"; Small **10** (16) 3347 (2014).
81. Yuhua Xue, Janice M. Baek, Hao Chen, Jia Qu, and Liming Dai; "N-doped graphene nanoribbons as efficient metal-free counter electrodes for disulfide/thiolate redox mediated DSSCs"; Nanoscale, **7**, 7078 (2015).
82. Zegao Wang, Pingjian Li, Yuanfu Chen, Jiarui He, Jingbo Liu, Wanli Zhang, Yanrong Li; "Phosphorus-doped reduced graphene oxide as an electrocatalyst counter electrode in dye-sensitized solar cells"; Journal of Power Sources, **263**, 246 (2014).
83. Yedi Xing, Xiaojia Zheng, Yihui Wu, Mingrun Li, Wen-Hua Zhang, and Can Li; "Nitrogen-doped carbon nanotubes with metal nanoparticles as counter electrode materials for dye-sensitized solar cells"; Cite this: DOI: 10.1039/c5cc01379h.

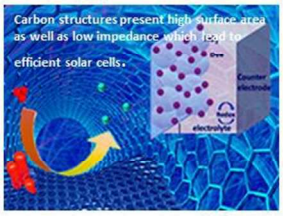

254x190mm (96 x 96 DPI)